

shape of the curve but values of  $L_a$  that closely matched that determined from lifetime measurements.

Both Lampert's theory and that of I predict that the carrier concentration in the center of the intrinsic region should be approximately proportional to  $J^{2/3}$ . This is equivalent to stating that  $\eta_0$  is constant. In the detailed treatment of I, it is shown that  $\eta_0$  is a slowly varying function of  $J$  in voltage regions where the current does not deviate strongly from the  $V^3$  relationship.

The carrier concentration at the junctions agrees with the theory only insofar as the concentrations are proportional to the current density. The explanation for the variation in concentration in different units at any current level is not understood at present.

In general, it is felt that Lampert's prediction of the influence of double injection on the current-voltage characteristics was confirmed. Both the theoretical treatment in I and the experimental work reported here

point up the fact that carrier diffusion effects must be considered in any detailed analysis.

*Note added in proof.* The values of the hole and electron mobilities used in this paper were 360 and 1600  $\text{cm}^2/\text{V sec}$ , respectively. Better values of the mobilities are 475 and 1325  $\text{cm}^2/\text{V sec}$ . [G. W. Ludwig and R. L. Watters, *Phys. Rev.* **101**, 1699 (1955).] This represents only an 8% change in the product of the mobilities (used to calculate the current-voltage characteristic) and also in the sum of the mobilities (used to calculate the carrier densities). This change in no way alters the conclusions of the paper.

#### ACKNOWLEDGMENT

The authors acknowledge with pleasure the assistance of H. L. Dunlap whose careful preparation of the samples was in a large degree responsible for the success of the measurements.

## Interpretation of Potential-Probe Measurements in Two-Carrier Structures

J. W. MAYER, O. J. MARSH, R. BARON, R. KIKUCHI, AND J. M. RICHARDSON

*Hughes Research Laboratories, Malibu, California*

(Received 20 July 1964)

Theoretical arguments and experimental evidence show that the potential  $\phi$ , measured by a high-impedance metal probe to the surface of a semiconductor or insulator in which the electron and hole concentrations are nearly equal, is given by  $\phi = (\mu_n \phi_n + \phi_p \mu_p) / (\mu_n + \mu_p)$ , where  $\phi_n$  and  $\phi_p$  are the electron and hole quasi Fermi levels and  $\mu_n$  and  $\mu_p$  are the electron and hole mobilities. As a consequence, the carrier concentration  $n$  is given exactly by  $n = |J / [e \mu_p (b+1) d\phi/dx]|$  where  $J$  is the current density. This relation constitutes a powerful tool for measuring  $n$ . The experimental evidence was found from measurements on silicon *p-i-n* structures forward biased into the double injection region where  $n \approx p$ . The observed potential drops  $\Delta V$  at the *p-i* and *n-i* junctions were compared with the values of the carrier concentrations  $n_1$  at the junctions. The theoretical relation between  $\Delta V$  and  $n_1$  depends strongly on the assumption that  $\phi$  is the quantity measured by the probe. Thus the fact that the experimental data agree with the above mentioned theoretical relation is a strong confirmation of the use of  $\phi$ . Theoretical arguments suggest that the generalization to the case  $n \neq p$  is given by  $\phi = (n \mu_n \phi_n + p \mu_p \phi_p) / (n \mu_n + p \mu_p)$ .

### 1. INTRODUCTION

MEASUREMENT of the potential distribution in semiconductor and insulator structures by probe technique is useful in investigating the mobile-carrier and space-charge distribution. Previously, the interpretation of the probe potential has been possible only in moderately doped material. In this paper theoretical arguments are advanced to suggest an extension of the interpretation of the probe potential to the case where the influence of both carrier types must be considered. Experimental evidence is presented which confirms this extension for the case where  $n \approx p$  in the bulk of the material.

The interpretation of the measured probe potential is relatively straightforward in moderately doped semiconductor materials across which a voltage has been applied. In these cases, where the majority carrier dis-

tribution is relatively unperturbed, the potential distribution is related directly to the electrostatic potential.<sup>1-3</sup> The standard measurement technique is to use a finely pointed metal probe connected to a high-impedance voltmeter.<sup>4,5</sup> Macdonald<sup>3</sup> points out that in the one-carrier system, the potential probe measures the quasi Fermi level<sup>6</sup> potential of the mobile carriers, which is equivalent to measuring the electrostatic potential for the case where the majority carrier density is unperturbed.

<sup>1</sup> J. R. Macdonald, *Solid State Electron.* **5**, 11 (1962).

<sup>2</sup> J. R. Macdonald, *J. Chem. Phys.* **29**, 1346 (1958).

<sup>3</sup> J. R. Macdonald, *J. Chem. Phys.* **30**, 806 (1959).

<sup>4</sup> D. E. Sawyer, *Solid State Electron.* **5**, 89 (1962).

<sup>5</sup> W. Pearson, W. Read, and W. Shockley, *Phys. Rev.* **85**, 1055L (1952).

<sup>6</sup> See, for example, W. Shockley, *Electrons and Holes in Semiconductors* (D. Van Nostrand Co., Inc., New York, 1950), p. 308.

In the two-carrier case where the density of injected carriers is greater than the density of thermally generated carriers, the analysis is more complicated, involving the separate quasi Fermi levels of the holes and electrons.

In forward-biased *p-i-n* junctions it has been shown in the preceding paper<sup>7</sup> (hereafter referred to as II) that the injected carrier densities can exceed the thermally generated carrier densities by factors ranging from 1.5 to  $10^4$ . In the conductivity-modulated region, space-charge neutrality requires that  $n(x) \approx p(x)$  so that the quasi Fermi levels are equally displaced from their equilibrium position. It appeared then that the *p-i-n* junction structure would offer a means of verifying the interpretation of the probe potential in terms of the quasi Fermi levels rather than the electrostatic potential.

In Sec. 2 the theoretical interpretation of the probe measurement is discussed. The experimental procedure is discussed in Sec. 3, and the experimental results are presented in Sec. 4.

## 2. THEORY

### A. Probe Measurement

It has been shown by Shockley<sup>6</sup> that the current equations can be written in terms of the quasi Fermi levels  $\phi_n$  and  $\phi_p$  for electrons and holes. Following Shockley,  $\phi_n$  and  $\phi_p$  are defined in terms of the carrier concentrations  $n$  and  $p$  by

$$\begin{aligned} n &= n_i \exp[(\psi - \phi_n)/\beta]; & \phi_n &= \psi - \beta \ln(n/n_i), \\ p &= n_i \exp[(\phi_p - \psi)/\beta]; & \phi_p &= \psi + \beta \ln(p/n_i), \end{aligned} \quad (1)$$

where  $\psi$  is the electrostatic potential and is defined to coincide with the Fermi level under equilibrium conditions for intrinsic material, and  $\beta = kT/e$ .

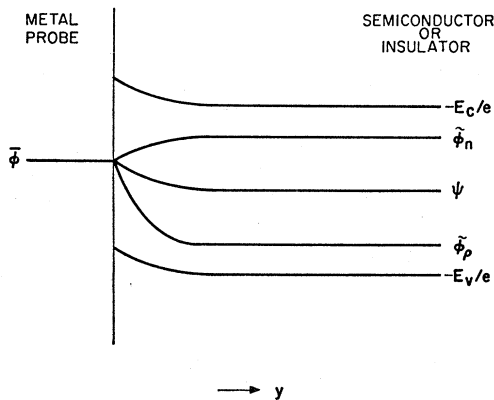


FIG. 1. Electron potential diagram at the interface of a metal probe and a semiconductor or insulator surface.

<sup>7</sup> J. W. Mayer, R. Baron, and O. J. Marsh, preceding paper, II, Phys. Rev. **137**, A286 (1965).

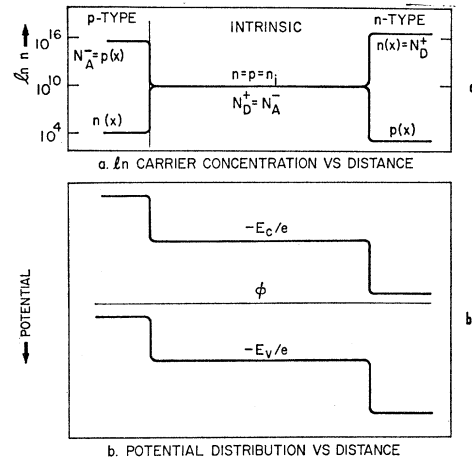


FIG. 2. (a) The spatial distribution of the carrier concentration of a *p-i-n* structure in thermal equilibrium. (b) The potential distribution for the case shown in (a).

The electron and hole current densities  $J_n$  and  $J_p$  can be written as

$$\begin{aligned} J_n &= -e\mu_n n \nabla \phi_n, \\ J_p &= -e\mu_p p \nabla \phi_p, \end{aligned} \quad (2)$$

where  $\mu_n$  and  $\mu_p$  are the electron and hole mobilities,  $n$  and  $p$  are the electron and hole densities, and  $e$  is the absolute value of the electronic charge.

The total current density  $J$  is the sum of  $J_p$  and  $J_n$  and is therefore written

$$J = -e\mu_p p \nabla \phi_p - e\mu_n n \nabla \phi_n. \quad (3)$$

If a metal probe is placed in contact with a semiconductor, the two quasi Fermi levels  $\phi_n$  and  $\phi_p$  merge into one level<sup>8</sup>  $\bar{\phi}$  in the metal as shown schematically in Fig. 1, where  $y$  denotes the direction perpendicular to the surface. On the semiconductor side near the contact, the carrier densities differ from the values in the bulk; the change of  $n(y)$  and  $p(y)$  is reflected in the sharp variation of  $\phi_n$  and  $\phi_p$  near the probe contact.  $\bar{\phi}_n$  and  $\bar{\phi}_p$  denote the values of the quasi Fermi level, and  $\bar{n}$  and  $\bar{p}$  the carrier densities, for the bulk of the material far away from the probe.

It is reasonable to assume that the currents flowing to the probe are radial sufficiently near the probe. Restricting the following to a one-dimensional argument, the  $y$  components of  $J_n$  and  $J_p$  along the  $y$  axis contain only the currents flowing to the probe and can be written as

$$\begin{aligned} J_n^y &= -e\mu_n n (d\phi_n/dy), \\ J_p^y &= -e\mu_p p (d\phi_p/dy). \end{aligned}$$

Because of the assumption that the probe draws no

<sup>8</sup> The assumption that  $\phi_n$  and  $\phi_p$  merge smoothly together without any discontinuity at the boundary makes possible the simple theoretical arguments in this paper. However, theoretical considerations indicate that the extremely small diffusion length for holes in the metal would make any discontinuity negligibly small.

current, it follows from the above that  $J^y=0$  and  $J_n^y = -J_p^y = J_1(y)$  everywhere on the  $y$  axis. Multiplying these equations by  $\tilde{n}/n$  and  $\tilde{p}/p$ , respectively, and integrating along the  $y$ -axis from  $y=0$  at the contact to  $y=d$  (where  $d$  is large enough that  $\phi_n = \tilde{\phi}_n$  and  $\phi_p = \tilde{\phi}_p$ ) in the interior of the semiconductor, one obtains

$$\int_0^d \tilde{n}(J_n^y/n)dy = -e\mu_n\tilde{n}(\tilde{\phi}_n - \bar{\phi}), \tag{4}$$

$$\int_0^d \tilde{p}(J_p^y/p)dy = -e\mu_p\tilde{p}(\tilde{\phi}_p - \bar{\phi}).$$

Adding the two expressions and dividing the sum by  $e(\tilde{n}\mu_n + \tilde{p}\mu_p)$ , one obtains

$$\bar{\phi} - \frac{\mu_n\tilde{n}\tilde{\phi}_n + \mu_p\tilde{p}\tilde{\phi}_p}{\tilde{n}\mu_n + \tilde{p}\mu_p} = \Delta, \tag{5}$$

where

$$\Delta \equiv \frac{1}{e(\tilde{n}\mu_n + \tilde{p}\mu_p)} \int_0^d \left( \frac{\tilde{n}J_n^y}{n} + \frac{\tilde{p}J_p^y}{p} \right) dy. \tag{6}$$

In order to interpret the probe voltage  $\bar{\phi}$  in terms of material parameters, it is necessary to estimate the value of  $\Delta$ . This will require the use of several assumptions. By using the relations  $J^y=0$  and  $\tilde{n} \approx \tilde{p}$ , Eq. (6) may be written as

$$\Delta = \frac{1}{e(\mu_n + \mu_p)} \int_0^d \frac{[n(y) - p(y)]J_1(y)}{n(y)p(y)} dy. \tag{7}$$

Thus, if the net charge  $n-p$  is sufficiently small compared with the product  $np$ ,  $\Delta$  can be small compared with  $\bar{\phi} - \tilde{\phi}_n$  or  $\bar{\phi} - \tilde{\phi}_p$  and we can approximate from (5) that

$$\bar{\phi} \approx (\mu_n\tilde{\phi}_n + \mu_p\tilde{\phi}_p) / (\mu_n + \mu_p) = (b\tilde{\phi}_n + \tilde{\phi}_p) / (b+1), \tag{8}$$

where  $b = \mu_n/\mu_p$ . As can be seen from (5),  $\Delta$  must be negligible in the case of an extrinsic semiconductor where the majority carrier density is much greater than the minority carrier density if the probe voltage is to measure the quasi Fermi level of the majority carriers as suggested by Macdonald.<sup>1</sup> This suggests that it might be reasonable to assume that  $\Delta$  is negligible for all cases, and that the probe potential can be interpreted as the mobility-weighted mean of the quasi Fermi levels. A more rigorous evaluation of  $\Delta$  is being treated by Kikuchi.

The remainder of this paper presents, for the case where  $\tilde{n} \approx \tilde{p}$ , strong experimental evidence supporting the validity of (8).

### B. *p-i-n* Structure

In order to discuss the experimental data it is necessary to review some of the characteristics of a forward-biased *p-i-n* structure. The spatial distribution of the

carrier concentration and potential for a *p-i-n* structure in thermal equilibrium is shown in Fig. 2. In the intrinsic region where  $N_d^+ = N_A^-$ , the concentrations of holes and electrons are equal to the intrinsic concentration  $n_i$ . The increase in electrons from  $n_i$  to  $n = N_D^+$  at the *n-i* junction and holes from  $n_i$  to  $p = N_A^-$  at the *p-i* junction is reflected in the curvature of the bands at the junctions. The width of the region over which the curvature occurs is approximately equal to the Debye length

$$X_0 = (\beta\epsilon/4\pi en_i)^{1/2}, \tag{9}$$

which for silicon at room temperature is about 20  $\mu$ . The distribution of the carrier concentration and potential in a forward-biased *p-i-n* junction is shown in Fig. 3. In the intrinsic region, consideration of space-charge neutrality requires that  $n(x) \approx p(x) > n_i$ . The injected carrier densities may exceed the intrinsic carrier concentration by a factor of 1.5 to  $10^4$ . As discussed in II, the carrier distributions are characterized by an exponential decrease from the *n-i* and *p-i* junctions that may be approximated by a factor  $\exp(x/L_a)$  where  $L_a$  is the ambipolar diffusion length given by  $L_a = [2D_n\tau/(b+1)]^{1/2}$ . Here  $D_n$  is the electron diffusion constant and  $\tau$  is the common high level lifetime. The carrier concentration in the central portion of the intrinsic region varies more weakly, typically a factor of 10-100 less than the concentration at the *n-i* and *p-i* junctions.

These variations in carrier concentration are reflected in the variation of the quasi Fermi levels  $\phi_n$  and  $\phi_p$  shown in Fig. 3(b). The weighted average of the quasi Fermi levels  $\bar{\phi}$  has the same general shape of  $\phi_n$  or  $\phi_p$  except at the junctions where there is a relatively steep step. The width of the step is determined by the Debye

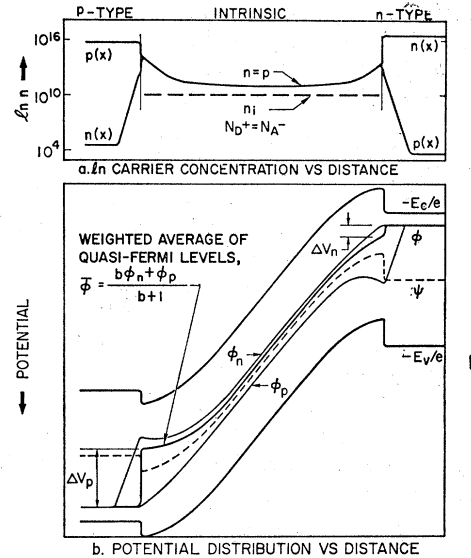


FIG. 3. (a) The spatial distribution of the carrier concentration in a forward-biased *p-i-n* structure. (b) The potential distribution for the case shown in (a), showing the influence of  $\bar{\phi}$  on  $\Delta V_n$  and  $\Delta V_p$ .

length. Note that the value of  $n$  to be used in the formula for the Debye length is that given by the carrier concentration at the junction  $\tilde{n}_1$ . Thus the width of the step will decrease with increasing injection level. Applying the definition of the quasi Fermi levels, Eq. (1), and Eq. (8) to the bulk

$$\bar{\phi} - \psi = -\beta[(b-1)/(b+1)] \ln(\tilde{n}_1/n_i), \quad (10)$$

where  $\tilde{n}_1$  is the value of  $n$  at the junction away from the probe.

Assuming that Boltzmann statistics apply across the junction, the voltage step that the probe would measure if it measured  $\psi$  rather than  $\bar{\phi}$  is given by

$$\begin{aligned} \Delta V_{p,n}(EP) &= \phi_p^* - \psi = \psi - \phi_n^* \\ &= \beta \ln(\tilde{n}_1/n_i) \end{aligned} \quad (11)$$

for both the  $p$ - $i$  and  $n$ - $i$  junctions. Here  $\phi_p^*$  and  $\phi_n^*$  are the quasi Fermi levels for the majority carriers in the appropriate regions and  $\tilde{n}_1$  is measured at the appropriate junction. On the other hand, when the probe measures  $\bar{\phi}$  rather than  $\psi$ , the step  $\Delta V_p$  at the  $p$ - $i$  junction is given by [using (10) and (11)]

$$\begin{aligned} \Delta V_p(QFL) &= \phi_p^* - \bar{\phi} \\ &= [2b/(b+1)]\beta \ln(\tilde{n}_1/n_i), \end{aligned} \quad (12)$$

and the step  $\Delta V_n$  at the  $n$ - $i$  junction is given by

$$\begin{aligned} \Delta V_n(QFL) &= \bar{\phi} - \phi_n^* \\ &= [2/(b+1)]\beta \ln(\tilde{n}_1/n_i). \end{aligned} \quad (13)$$

The potential probe measurement on a forward-biased  $p$ - $i$ - $n$  junction will be characterized by:

1. A step in voltage  $\Delta V_n$  and  $\Delta V_p$  at the  $n$ - $i$  and  $p$ - $i$  junctions. If the carrier concentrations at the  $n$ - $i$  and  $p$ - $i$  junctions are approximately equal, then  $\Delta V_p = b\Delta V_n$ .
2. A variation of the potential with distance near the  $n$ - $i$  and  $p$ - $i$  junctions which is related to the exponential decrease in carrier concentration.

The relationship between the probe potential and carrier concentration in the bulk can be found from (3) as follows. Since (3) is general, it can be applied to the current in the bulk. Indicating the quantities in the bulk with tildes, one can write (3) as

$$\tilde{\mathbf{J}} = -e\mu_p\tilde{p}\nabla\tilde{\phi}_p - e\mu_n\tilde{n}\nabla\tilde{\phi}_n. \quad (14)$$

It should be noted that  $\tilde{\mathbf{J}}$  is the current flowing in the bulk of the sample and is different from  $J(y)$  used in Sec. 2A to indicate the current flowing toward the metal probe. When  $\tilde{\mathbf{J}}$  flows in the  $x$  direction, and when  $\tilde{n}(x) = \tilde{p}(x)$ , one can simplify Eq. (14) with the help of Eq. (10) as

$$\tilde{\mathbf{J}} = -e\mu_p(b+1)\tilde{n}(x)[d\bar{\phi}(x)/dx].$$

This shows that by measuring  $\bar{\phi}(x)$  and  $\tilde{\mathbf{J}}$ , one can derive the carrier concentration  $\tilde{n}(x)$  from

$$\tilde{n}(x) = |J(e\mu_p(b+1)[d\bar{\phi}(x)/dx]^{-1})|. \quad (15)$$

### 3. EXPERIMENTAL PROCEDURE

In the fabrication of the  $p$ - $i$ - $n$  junctions, the basic techniques of Pell<sup>9</sup> were followed. A more detailed description of the procedure used in this investigation can be found in the paper by Mayer<sup>10</sup> and in II.

The intrinsic widths after drift ranged from 0.2 to 5 mm. The units were cut into 3×3-mm samples with all but 1–2 mm of the undrifted  $p$ -type material removed. The samples were etched with a 4-4-5 solution [four parts by volume HNO<sub>3</sub> (70%) to four parts HF (48%) to five parts glacial acetic acid] and then lapped with 0.1- $\mu$  grit (or polished) to produce parallel faces on the sides. Gallium contacts were applied to the  $n$ - and  $p$ -type regions by friction tinning.

The sample lifetime was measured by biasing the sample into the  $V^3$  portion of the current-voltage characteristic, and measuring the current decay after excitation by a brief intense flash of light which was incident on the sample through a  $\frac{1}{8}$ -in. silicon filter. The lamp (Microflash Model 550) decay time was less than 2  $\mu$ sec. The lifetime values were determined from the initial exponential time constant of decay; the measured values ranged between 14 and 100  $\mu$ sec.

The units were then mounted in a fixture so that a potential traverse could be made. The samples are held rigidly with one end grounded and the other contact connected to the voltage supply and current meter. The tungsten potential probe which is sharpened by electroforming is held by a three-axis micromanipulator. The smallest reproducible distance increment was 0.01 mm.

The probe was weighted and held in a stainless-steel sleeve which permitted vertical motion so that the same pressure was exerted on the sample by the probe for each measurement. Examination of the silicon surface after repeated measurements indicated that the probe did not damage the surface. The probe was connected to a high-input impedance voltmeter, either GR Model 1230A or Hallex Model 302E. The input impedance of the probe was sufficiently high that measurement of the probe potential did not affect the current through the sample.

It was found that a lightly lapped or polished surface (as opposed to an etched surface) gave the most consistent and reproducible results. The potential probe measurements on an etched surface coincided with those on a lapped surface when the sample was biased far into the conductivity-modulated regime. However, anomalous results were found in the low bias regions. All the experimental results reported herein were obtained on a lightly lapped surface.

### 4. EXPERIMENTAL RESULTS

Over 50 samples were fabricated for this study and the work reported in the previous paper. Of these, 20 units were evaluated quantitatively. Detailed poten-

<sup>9</sup> E. M. Pell, J. Appl. Phys. **31**, 291 (1960).

<sup>10</sup> J. W. Mayer, J. Appl. Phys. **33**, 2894 (1962).

tial probe measurements at room temperature were made on eight units whose carrier-lifetime values, intrinsic-region length, and current-voltage characteristics were representative of the total group of units. An experimental constraint on the choice of units arose from the fact that compensation in the drifted region degraded because of lithium-ion motion in units held at high forward-bias voltages during potential probe measurements. To reduce this effect, samples were chosen which exhibited conductivity modulation effects at applied voltage between 5 and 30 V. As a further precaution, potential traverses were made on the samples biased in the low-voltage Ohmic conduction region before and after each series of potential traverses. Any departure from linearity of these traverses would indicate a degradation of the compensated intrinsic region.

Two potential-probe traverses representing typical experimental results are shown in Fig. 4 for unit 0-1-4. The positions of the *p-i* and *n-i* junctions are shown. The linear increase in probe potential for the measurement taken at 0.3 V applied (where the sample is in the Ohmic conduction region) indicates the high degree of compensation of the drifted region. In this case the applied electric field is constant over the drifted region. The solid line shows the marked distortion in the potential distribution near the junctions that occurs when the sample is in the conductivity modulated region of the current-voltage characteristic. The voltage steps  $\Delta V_p$  and  $\Delta V_n$  near the *p-i* and *n-i* junction are evident. In all units measured,  $\Delta V_n$  was less than  $\Delta V_p$ .

More detailed measurements of the potential distribution near the *p-i* junction of 0-1-4 are shown in

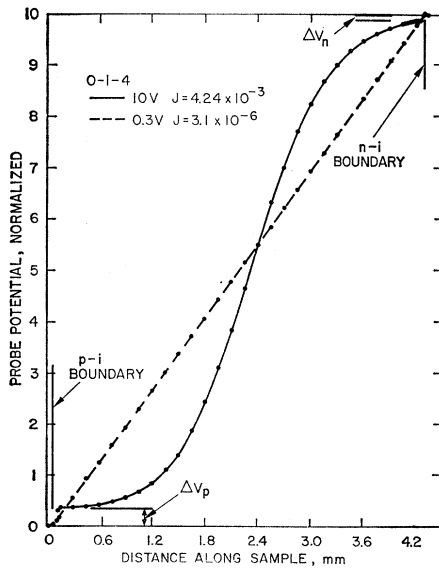
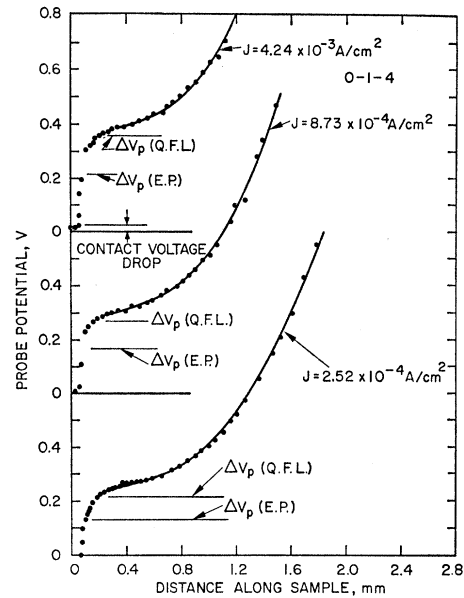
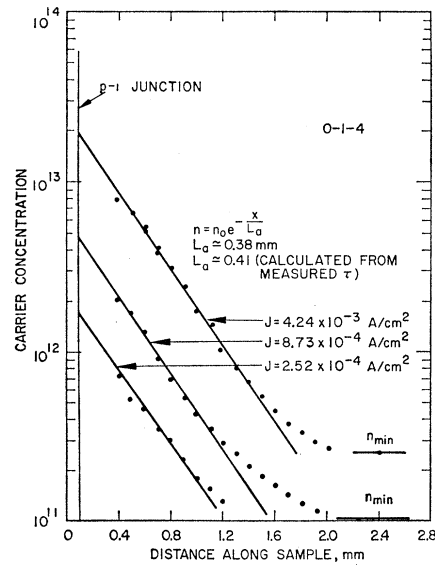


FIG. 4. The measured normalized probe potential versus distance along the sample for two applied biases, 0.3 V in the ohmic region and 10 V in the  $I \propto V^3$  region. The curves are smooth curves drawn through the experimental points. Note that current densities are given in amperes per square centimeter.



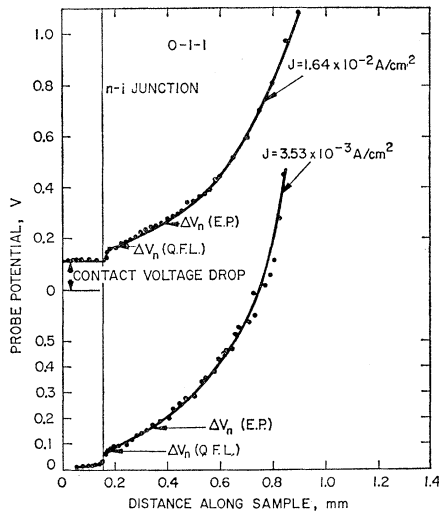
(a)



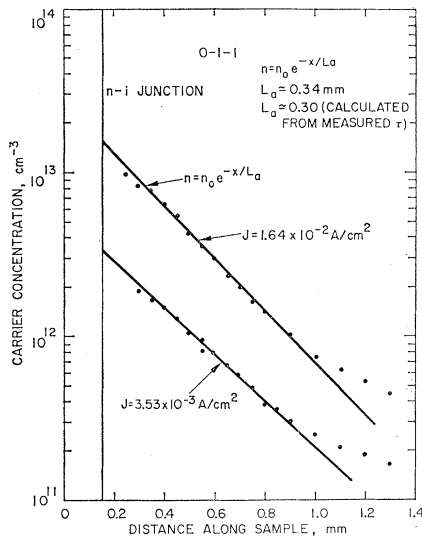
(b)

FIG. 5. (a) Detail of the measured probe potential versus distance along sample 0-1-4 near the *p-i* junction for three values of the current density.  $\Delta V_p(QFL)$  and  $\Delta V_p(EP)$  were calculated from the values of  $n$  in Fig. 5(b) extrapolated to the junction and Eqs. (12) and (11), respectively. (b) Detail of the carrier concentration versus distance along sample 0-1-4 near the *p-i* junction, calculated from Eq. (15) and the measured probe potential. Here,  $n_0$  is a constant of proportionality.

Fig. 5(a) for three values of the sample current. The width of the potential step decreased with increased carrier injection levels as was found in all samples and as predicted by the decrease in the Debye length mentioned above. A potential drop at the contact between the gallium and *p*-type material can be seen at the highest current level.



(a)



(b)

FIG. 6. (a) Detail of the measured probe potential versus distance along sample 0-1-1 near the *n-i* junction for two values of the current density.  $\Delta V_n(QFL)$  and  $\Delta V_n(EP)$  were calculated from the values of  $n$  in Fig. 6(b) extrapolated to the junction and Eqs. (13) and (11), respectively. (b) Detail of the carrier concentration versus distance along sample 0-1-1 near the *n-i* junction, calculated from Eq. (15) and the measured probe potential. Here,  $n_0$  is a constant of proportionality.

The carrier distributions shown in Fig. 5(b) were obtained graphically at each point shown by drawing the tangent line to the potential distribution at the point and then using the relationship shown in Eq. (15). The exponential decrease in carrier concentration agrees closely with that predicted by the ambipolar diffusion length as calculated from the measured carrier lifetime. The well-defined exponential nature of the carrier distribution makes it possible to determine the carrier concentration by extrapolation to the *p-i* junction.

Using these values of the carrier concentration,  $\Delta V_p$  was calculated using Eq. (12). These values, which are shown in Fig. 5(a) marked  $\Delta V_p(QFL)$ , agree closely with the measured step. The values for the step calculated from Eq. (11) on the basis of the change in electrostatic potential, denoted  $\Delta V_p(EP)$ , are shown for comparison in Fig. 5(a).

Fig. 6(a) shows the potential distribution near the *n-i* junction in sample 0-1-1. The voltage step is clearly outside experimental error. The carrier distribution for the same two current values is shown in Fig. 6(b). Again there is good agreement with the exponential decrease predicted by the ambipolar diffusion length. The values of  $\Delta V_n(QFL)$  and  $\Delta V_n(EP)$  calculated from the extrapolated values of the carrier concentration at the *n-i* junction are shown in Fig. 6(a).

In six samples, the carrier distribution followed the exponential decrease over a sufficient range of concentration to permit extrapolation to the junctions. The values of  $\Delta V$  could be determined from the value of the measured probe potential at the "knee" of the potential distribution with an uncertainty of  $\pm 0.02$  V. The values of the carrier concentration at the *n-i* and *p-i* junction are shown in Fig. 7 as a function of the potential step  $\Delta V$ . The calculated values of  $\Delta V$ , both using the weighted average of the quasi Fermi levels and using the change in electrostatic potential, are denoted by solid and dashed lines in Fig. 7. The experimental points are in close agreement with the values of  $\Delta V$  calculated from the quasi Fermi level.

It should be noted here that for these samples, the maximum value of  $d\tilde{n}/dx$  was small enough to be

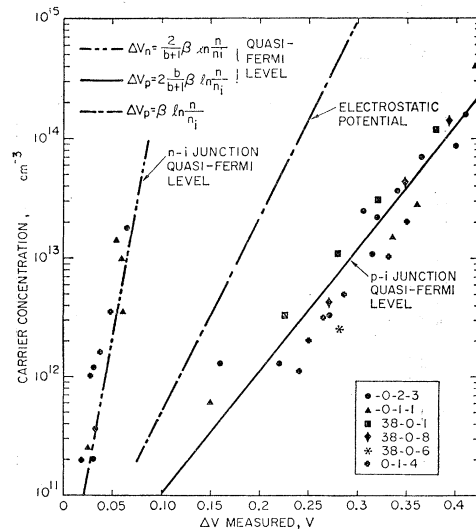


FIG. 7. Plot of the measured values of the carrier concentration at the *p-i* and *n-i* junctions versus the potential drop  $\Delta V$  at the same junction. The straight lines represent, from left to right, the theoretical relations in Eqs. (13), (11), and (12).

neglected in the current equation, so that

$$\frac{d\bar{\phi}}{dx} = \frac{d\psi}{dx} - \beta \frac{b-1}{b+1} \frac{d\bar{n}}{\bar{n} dx} \approx \frac{d\psi}{dx}$$

from (10); Eq. (15) gives the same value for  $\bar{n}(x)$  whether the probe measured  $\psi$  or  $\bar{\phi}$ . Since the  $\Delta V$  are direct experimental quantities and since the calculation of the  $\bar{n}_1$  from direct experimental quantities does not depend on the assumption to be checked, the experimental relation between  $\Delta V$  and  $\bar{n}_1$  can be used to establish the validity of a theoretical relation and therefore of the assumption on which it is based.

Thus, the close agreement of the experimental data with the theoretical relations given in (12) and (13), and the violent disagreement with the theoretical relations given in (11) strongly confirm that the probe measures  $\bar{\phi}$  and not  $\psi$  for the case  $n \approx p$ .

It is fortunate that  $\Delta V$  is so sensitive to what the probe measures; the fact that  $d\bar{n}/dx$  is negligible also means that the observed exponential form of  $n(x)$  near the contacts is not sensitive to what the probe measures. Only for much higher injection levels where  $\bar{n}_1$  is large enough so that  $d\psi/dx \approx \beta(b-1)/L_a(b+1)$  can the form of  $n(x)$  be used to determine what the probe measures.

It should also be noted that the choice of ion-drifted  $p$ - $i$ - $n$  junctions was particularly fortunate in that the interface between intrinsic region and the low resistivity  $n$ - and  $p$ -type material was well defined. The ionized impurity distributions in well-compensated units can be approximated by a step function.<sup>9</sup> The width of the potential step, then, can be determined by the Debye length, which is small in intrinsic silicon ( $\approx 20 \mu$  at  $RT$ ). In addition, because of good injection efficiency in the  $p$ - $i$ - $n$  structure, the carrier distribution near the junction behaved exponentially with distance; this permitted determination of the carrier concentration at the junction by extrapolation. This, along with the small scatter in the potential measurements, made possible accurate measurements of  $\bar{n}_1$  and  $\Delta V$ .

## 5. CONCLUSIONS

The close correlation between the calculated and experimental values of the potential step at the junctions is strong evidence that the potential probe

measurement has been correctly interpreted in terms of the weighted average of the quasi Fermi levels as suggested by the theoretical arguments. It should be noted that the experimental data apply to the case where  $n \approx p$ .

This determination of what the probe measures permits the use of the relation between  $\bar{n}(x)$  and  $\bar{\phi}(x)$  presented in (15) as a powerful method of determining the carrier distribution. This is especially true since the potential distribution can easily be measured on a well-prepared surface.

The theoretical justification for the interpretation of the potential probe measurement is not on firm footing. The argument that the  $\Delta$  term in (5) adds a negligible contribution to the value of  $\bar{\phi}$  can be treated in a qualitative manner for the case where  $n \approx p$  and the probe current is zero. Attempts at a more rigorous solution have shown that  $\Delta$  depends on the values of  $\phi_n$ ,  $\phi_p$  and the electrostatic potential at the probe to semiconductor interface as well as their spatial configuration. However, in view of the strong experimental evidence presented in the case of  $\bar{n} \approx \bar{p}$ , it is reasonable to assume that the probe voltage  $\bar{\phi}$  can be interpreted on the basis that

$$\bar{\phi} = (\bar{n}\mu_n\bar{\phi}_n + \bar{p}\mu_p\bar{\phi}_p) / (\bar{n}\mu_n + \bar{p}\mu_p) \quad (16)$$

for all  $\bar{n}$  and  $\bar{p}$ .

When the majority carrier concentration is much greater than that of the minority carriers (i.e., in heavily doped material), Eq. (16) correctly reduces to the prediction that the probe measures the quasi Fermi level of the majority carrier.<sup>1</sup> In the case where  $n \approx p$ , this reduces to (10), which predicts that the probe measures the average of the quasi Fermi levels weighted with the mobilities.<sup>11</sup>

## ACKNOWLEDGMENT

The authors acknowledge the contribution of H. L. Dunlap who fabricated the samples.

<sup>11</sup> *Note added in proof:* The values of the hole and electron mobilities used in this paper were 360 and 1600 cm<sup>2</sup>/Vsec, respectively. Better values of the mobilities are 475 and 1325 cm<sup>2</sup>/Vsec. [G. W. Ludwig and R. L. Watters, Phys. Rev. **101**, 1699 (1955)]. This represents only an 8% change in value of the sum of the mobilities (used to calculate carrier densities), but does represent a larger change in the ratio of mobilities. The use of the new mobility values in no way alters the conclusions of the paper.